УЧЕНЫЕ ЗАПИСКИ КАЗАНСКОГО УНИВЕРСИТЕТА.
СЕРИЯ ЕСТЕСТВЕННЫЕ НАУКИ

2024, Т. 166, кн. 2
С. 210–228

ISSN 2542-064X (Print)
ISSN 2500-218X (Online)

ORIGINAL ARTICLE

UDC 546.05

doi: 10.26907/2542-064X.2024.2.210-228

Anomalous Conductive Properties of Polymer Composites with Carbon Nanotubes: Why Power Laws Are Not Universal

T.L. Khamidullin[a], I.V. Lounev[a], S.A. Sattarov[b], A.M. Dimiev[a]

[a]*Kazan Federal University, Kazan, 420008 Russia*
[b]*Jizzakh Polytechnical Institute, Jizzakh, 130100 Republic of Uzbekistan*

Abstract

The conductive properties of CNT/polymer composites have been extensively studied. However, the impact of CNT distribution in the matrix on the composite polarization remains underexplored and poorly understood. Since it is difficult to achieve a uniform distribution of CNTs in polymers, most researchers have focused only on indiscriminately aggregated states. In this article, a new blending method was suggested to prepare a series of epoxy resin-based composite samples with varying levels of CNT uniformity/aggregation and the same filling fractions. Notably, the permittivity values turned out to be inversely related to the composite uniformity: the lowest permittivity values were obtained in the most uniform formulation, and vice versa. With 0.1% CNT, the real part values of the most uniform and aggregated samples were 6.6 and 16.2 at 10^7 Hz and 11.6 and 370.5 at 10^1 Hz, respectively. For the filler content of 0.1–0.5%, the conductive properties were largely determined by the distribution of CNTs and not their content. Within the entire frequency range, the uniform sample with 0.2% CNT exhibited significantly lower permittivity than the aggregated sample with 0.1% CNT. These findings emphasize the importance of the aggregation factor and underscore the non-universality and limitations of the percolation theory and power laws. The observed phenomenon is best explained by the micro-capacitor model, or the Maxwell–Wagner polarization, and suggests that a significant portion of the literature in the field needs to be reconsidered.

Keywords: epoxy resin composites, carbon nanotubes, interfacial polarization, permittivity, aggregation, microcapacitor model

Introduction

The permittivity of dielectric materials is their ability to interact with electromagnetic radiation, which must be controlled and adjusted for various applications, such as electromagnetic shielding, remote sensing, antennas, high-density energy storage, antistatic protection, self-heating, etc. Introducing conductive inclusions into the otherwise nonconductive polymer host is one of the simplest ways to enhance the permittivity of dielectric materials [1]. Among various types of conductive fillers, carbon nanostructures stand out for their unique properties and thus have gained a great deal of attention from the research community [2–4]. This is especially true for carbon nanotubes (CNTs) and graphene nanoribbons (GNRs) distinguished by high electrical conductivity and aspect ratio [5–13]. The latter property is the main reason for relatively low filling fractions needed to reach high permittivity values. However, despite

all advantages, CNTs have one inherent limitation when used as a filler: characterized by a very low affinity for most known polymers, they tend to aggregate in the polymer matrix [14], and, as a result, the properties of carbon/polymer composites become degraded. There is a strong consensus in the field that a more uniform distribution of CNTs yields better mechanical and conductive properties [14–16].

The underlying physics behind the electromagnetic behavior of dielectric composites remains elusive. Researchers have been trying to interpret their conductive properties through multiple theories and models. The percolation theory and power laws, which explain the macroscopic parameters of composites based on the statistical distribution of inclusions and predict a sharp increase in the tested property near the percolation threshold, are among the most widely employed ones [17–20]. They have proven to be a valuable tool in understanding the conductivity and permittivity of complex systems [17, 20, 21]. Although the power laws are popular and relatively accurate in describing certain complex materials, experiments have failed to verify their universality. Hence, the percolation threshold values for CNTs in composites are still a matter of debate. The reported values range from 0.002% to over 4% depending on CNT type, matrix composition, and processing techniques [22]. The problem is that the percolation theory ignores the chemical nature of the two phases, i.e., the cohesive forces between the host material and inclusions. In actual systems, when a liquid resin has a strong affinity for the inclusion material, it always wets the surface of the inclusion particles, creating a thin polymer layer between the neighboring particles, even at high filling fractions. Formally, the system will never reach true percolation in terms of DC conductivity. In modern literature, the term "percolation threshold" refers to the filling fractions at which the AC conductivity and/or permittivity exhibit a non-monotonous behavior with respect to the filler fraction [5, 23–27].

Alongside the percolation theory, the "microcapacitor model" has been recently introduced to explain the dielectric behavior of composites [9, 26–28]. This model considers composites as a network of microcapacitors distributed randomly in the dielectric host. In its essence this model is another wording for the interfacial polarization, often referred to as the Maxwell–Wagner polarization. Unlike the power laws, it provides a physical explanation for the observed phenomena with experimental support. For example, in our earlier study [29], we fabricated an anisotropic graphene/epoxy composite with the graphene layers arranged parallel to each other, resembling a battery of microcapacitors within the entire macroscopic sample. The permittivity values were significantly higher when measured in the direction where the 2D microcapacitor plates were arranged perpendicular to the applied electromagnetic field, i.e., similarly to the classical capacitor, compared to when they were aligned parallel. In case of the 1D CNTs, such anisotropy is less pronounced but detectable [15].

Several recent publications have emphasized the importance of the interface between CNTs and the matrix. In [9, 30], the CNT/polymer interfacial structure was modified using the covalent and non-covalent functionalization, resulting in the changes in conductivity/permittivity. The interface structure influences the charge accumulation and transfer through the interface, suggesting the need for more in-depth investigation. Nevertheless, in the available literature, the debates over this issue often lack scientific rigor [31, 32] and simply mention some "interface effect", which does not help in understanding the physical mechanisms of polarization.

There is not much research on how the aggregation of CNTs affects the conductive properties of composites. On the one hand, the aggregation has been actively discussed, and the common opinion is that a more uniform distribution is necessary to achieve higher permittivity values [9, 33], often through CNT functionalization. On the other hand, very few studies, if any, provide a direct comparison between samples with different levels of CNT aggregation at the same filler content. For example, Li et al. [22] examined the correlation between the degree of CNT aggregation and the percolation threshold. They developed a mathematical model for the relationship between the percolation threshold and the following two distribution parameters: "localized volume content of CNTs in an agglomerate" and "volume fraction of agglomerated CNTs." According to their model, the percolation threshold increases with the second parameter, but no straightforward conclusions were made about whether CNT aggregation leads to higher or lower permittivity values.

Many publications in the field ignore the impact of CNT aggregation on their results, and the vast majority of researchers explore materials containing CNTs in an indiscriminately aggregated state. One reason for this oversight may be the absence of straightforward methods to precisely control the degree of CNT aggregation while keeping all other parameters constant. Whereas aggregated samples are relatively easy to prepare, obtaining a non-aggregated uniform distribution is challenging.

In this study, we develop a method for controlling the distribution of CNTs in the epoxy resin matrix. Based on this method, we prepare a series of samples with varying but controlled degrees of uniformity/aggregation of CNTs in the polymer matrix at the same filler content. The resulting composites demonstrated significant differences in their permittivity values.

1. Material and Methods

1.1. Material. Tuball CNTs (batch #01RW02.N1.208) with a purity of > 80% and a catalyst content of < 15% were purchased from OCSiAl. The epoxy resin (NPEL-128, epoxy value 22.6, epoxide equivalent weight 186.2 g eq.$^{-1}$) from bisphenol-A and epichlorohydrin was obtained from Rus Chemicals Group (Russia). The hardener, polyethylene polyamine, was provided by Resurs Group (Russia). Isopropyl alcohol (IPA), graphite (the GL-1 grade), sulfuric acid, and potassium permanganate were supplied by TatKhimProduct (Russia). All commercial reagents and solvents were used as received without further purification.

1.2. Preparation of modified CNTs/epoxy composites

1.2.1. Oxidative modification of CNTs. CNTs (110.6 mg) were dispersed in 56.3 mL of concentrated sulfuric acid and stirred overnight using a magnetic stirrer. Then, 77.42 mg of potassium permanganate were added and stirred for 8 h. The reaction was quenched with ice made from deionized (DI) water. The mixture was centrifuged at 4000 rpm for 30 min in order to separate CNTs from the diluted acid. The precipitated CNTs were redispersed in a new portion of DI water, stirred for 1 h, and centrifuged again. These steps constituted one purification cycle. Four more purification cycles were performed consecutively. After the final precipitation, the as-washed CNTs were dried at ambient conditions. The as-obtained CNTs were denoted as modified CNTs (mCNTs).

1.2.2. Preparation of mCNT/epoxy formulations. mCNTs were dispersed in IPA using an ultrasonic bath. The temperature in the bath was maintained at 25–35 °C. It took about 3 h of sonication to achieve homogeneous dispersion with no particles discernible to the naked eye. The critical factor was the very low (0.015%) content of mCNTs in IPA. At this concentration, a homogeneous solution with no visible aggregates was obtained, which was not possible with higher concentrations. This solution was used to prepare samples with the "best" and "good" mCNT distribution. To prepare the formulations with the "bad" mCNT distribution, the initial diluted homogeneous solution was evaporated to reach the mCNT content of 0.5%. For the "worst" mCNT distribution, IPA was evaporated to reach the mCNT content of 3%. Subsequently, the as-prepared mCNT/IPA dispersions were blended with epoxy resin in certain proportions to reach the mCNT contents of 0.1, 0.2, and 0.5%. IPA was removed by evaporation at elevated temperature and reduced pressure with continuous stirring until constant weight. The formulations were sonicated in an ultrasonic bath at 80 °C for varying periods of time: 2 h for the best mCNT distribution, 30 min for the good mCNT distribution, and 5 min for the bad mCNT distribution. For the sample with the worst mCNT distribution, the formulation was not sonicated.

1.2.3. Curing the formulations. The curing was performed immediately after the sonication. First, the still hot formulation was degassed in a desiccator under reduced pressure for 20 min. Then, the hardener (polyethylene polyamine) was added in a weight ratio 10 : 1, and the mixture was blended manually and degassed again for 10 min. The degassed mixture was poured into molds and cured for 1 h at 60 °C followed by 2 h at 80 °C. For each tested formulation, three samples were prepared, and the measured permittivity values were almost the same for all of them.

1.3. Characterization of mCNTs and mCNT/epoxy formulations. The thermogravimetric analysis (TGA) of CNTs was performed with an STA 449 F5 Jupiter analyzer (Netzsch, Germany) in the argon atmosphere. Raman spectra of CNTs were acquired from the compressed powder sample using an ARS-3000 Raman microscope (Nano Scan Technology, Russia) equipped with the 532 nm excitation laser. The scanning electron microscopy (SEM) images were acquired with a Merlin high-resolution field-emission scanning electron microscope (Carl Zeiss, Germany) at an accelerating voltage of incident electrons of 5 kV and a current probe of 300 pA. The transmission electron microscopy (TEM) images were taken with a Hitachi HT7700 Excellence transmission electron microscope (Hitachi, Japan) at an accelerating voltage of 100kV in the TEM mode. The optical microscopy images were acquired from thin layers of the mCNT/epoxy formulations, sandwiched between a microscope slide and a cover slip, before adding the curing agent.

1.4. Dielectric measurements. The permittivity values were calculated from the capacitance measured with a Novocontrol BDS Concept-80 impedance analyzer (Novocontrol Technologies GmbH & Co. KG, Germany), with the automatic temperature control provided by the QUATRO cryo-system (temperature uncertainty ±0.5 °C). The samples were placed between two gold-plated electrodes of the capacitor. The capacitor was attached to the thermostated testing head. The measurements were conducted in the frequency range from 10^{-1} to 10^{7} Hz.

2. Results and Discussion

Most carbon-based materials, as stated above, have extremely low affinity for polymer matrices. The graphene oxide (GO)/epoxy resin system is a rare exception due to the high number of oxygen functional groups in the GO structure. Considering this property, the method of homogeneous liquid phase transfer (HLPT) of GO into epoxy resins has been introduced to ensure uniform distribution and fully exfoliated state of GO in the matrix [34]. The resulting GO distribution in epoxy resin leads to a significant transformation of the properties of both liquid formulations and solid polymer composites at extremely low filling fractions [35–37]. The strong affinity between GO and epoxy resin is the factor enabling it. To make carbon-based nanostructured materials compatible with epoxy resin, one needs to incorporate oxygen atoms into their structure. This was the strategy adopted in the present study to uniformly disperse CNTs in epoxy resin.

The oxidative modification of CNTs was performed with a $KMnO_4/H_2SO_4$ mixture, which is utilized in the Hummers graphite oxidation method. Complete oxidation, as outlined in the Hummers recipe, converts CNTs into a non-conductive material [38]. Hence, only a small amount of the oxidizer was added, i.e., 0.7 wt% eq. $KMnO_4$ relative to CNTs, as compared to 3–4 wt% eq. $KMnO_4$ used for the synthesis of GO and graphene oxide nanoribbons [39–41]. This oxidizer quantity was found to be optimal for achieving sufficient dispersibility of CNTs in epoxy resin and for simultaneously preserving their electrical conductivity. The characteristics of the modified CNTs (mCNTs) are shown in Fig. 1.

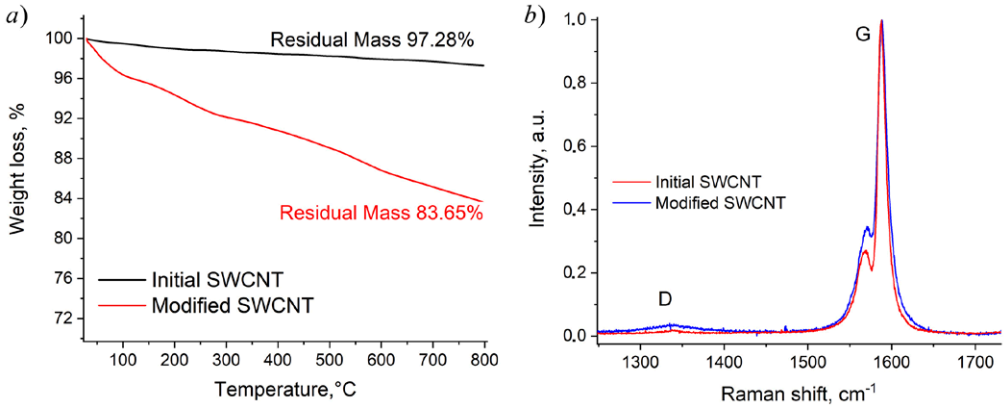

Fig. 1. Characteristics of mCNTs as compared to the original CNTs. *a*) TGA curves acquired in the argon atmosphere, *b*) Raman spectra acquired with a 533 nm excitation laser

The TGA of mCNTs revealed a weight loss of 16.3% at 800 °C (Fig. 1, *a*), which is much less than that for GO or oxidized graphene nanoribbons losing up to 55–60% of their original weight under similar conditions [38–42]. Notably, the TGA curve for mCNTs does not show a weight loss in the temperature range of 160–200 °C, which is characteristic of GO [43, 44]. The weight loss observed at the temperature above 300 °C is most likely associated with the removal of residual sulfuric acid trapped in the CNT bundles [38, 45], as well as with the decomposition of the catalyst-derived impurities, rather than with the decomposition of the oxygen groups. The Raman spectrum of mCNTs is very similar to that of the original CNTs (Fig. 1, *b*). The D-band is

only slightly enhanced, suggesting that the quantity of the introduced oxygen groups, serving as defects, was relatively low [46–48].

The Tuball CNTs analyzed in this study are very long and bundle with one another [49–52]. In the raw CNTs powder, there were CNT bundles with a diameter of 10–50 nm, consisting of tens of individual CNTs. The bundles could further twist to form secondary belt-like structures with a width up to 1 μm (Fig. 2, *a*). After the sonication in IPA, the secondary structures were easily untwisted to the primary bundles (Fig. 2, *b*). The primary CNT bundles are stable enough to resist isolation into individual CNTs until prolonged sonication of the dispersions with a low CNT content in aqueous surfactant solutions [51, 52]. Following the simple sonication in IPA, CNTs remained bundled (Fig. 2, *b*). After the oxidative modification, mCNTs retained their bundled state as well (Fig. 2, *c*). Thus, the smallest structural unit of CNTs in epoxy resin is a bundle with a diameter of 10–30 nm.

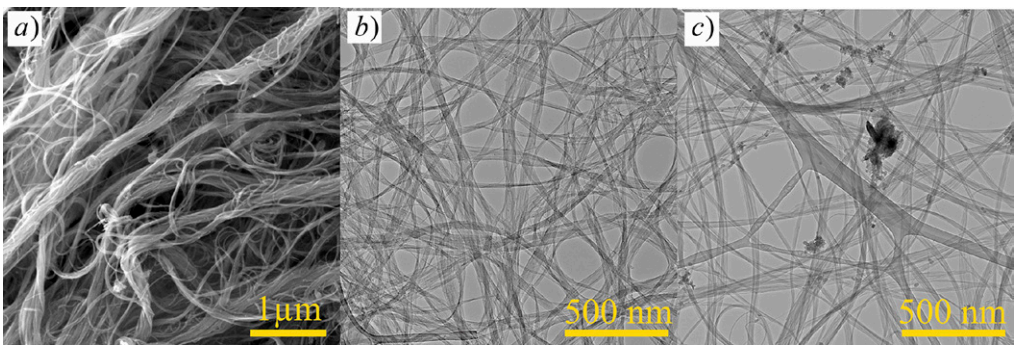

Fig. 2. Electron microscopy images of the original CNTs (*a*, *b*) and mCNTs (*c*). SEM image (*a*) and TEM images (*b*, *c*).

To incorporate mCNTs into epoxy resin, the HLPT method [34] was used. The degree of mCNT aggregation was controlled through the concentration of the mCNT/IPA dispersion and the time of sonication of the dispersion in hot epoxy resin after the blending. Overall, composites with three different mCNT contents in the matrix were obtained: 0.1, 0.2, and 0.5%, respectively. The mCNT content is hereinafter expressed as a weight percentage. For 0.1% mCNT, four types of composites with varying degrees of mCNT aggregation, from the most uniform distribution to the most aggregated state, were prepared. The respective samples were labeled as 0.1-best, 0.1-good, 0.1-bad, and 0.1-worst, in ascending order of the aggregation degree.

In Fig. 3, the optical microscopy images of the four uncured liquid CNT/epoxy formulations are given. The 0.1-best sample looks like clear epoxy resin (Fig. 3, *a*). However, even in this sample, mCNTs were thin bundles, as they appear in Fig. 2, *c*. These bundles were < 30 nm thick and thus undetectable by optical microscopy. Despite being invisible, mCNTs were still present in the resin. When the liquid formulation was left to stay for 30 min at 80 °C, mCNTs began to gradually agglomerate in the resin in the form of foggy patches (Fig. 4). The 0.1-good sample (Fig. 3, *b*) looked similar to 0.1-best sample after standing for 30 min at 80 °C. In addition to foggy agglomerates, the 0.1-bad sample contained large aggregates (up to 200 μm) comprising multiple CNT bundles (Fig. 3, *c*). The 0.1-worst sample prepared without sonication had numerous large aggregates (Fig. 3, *d*).

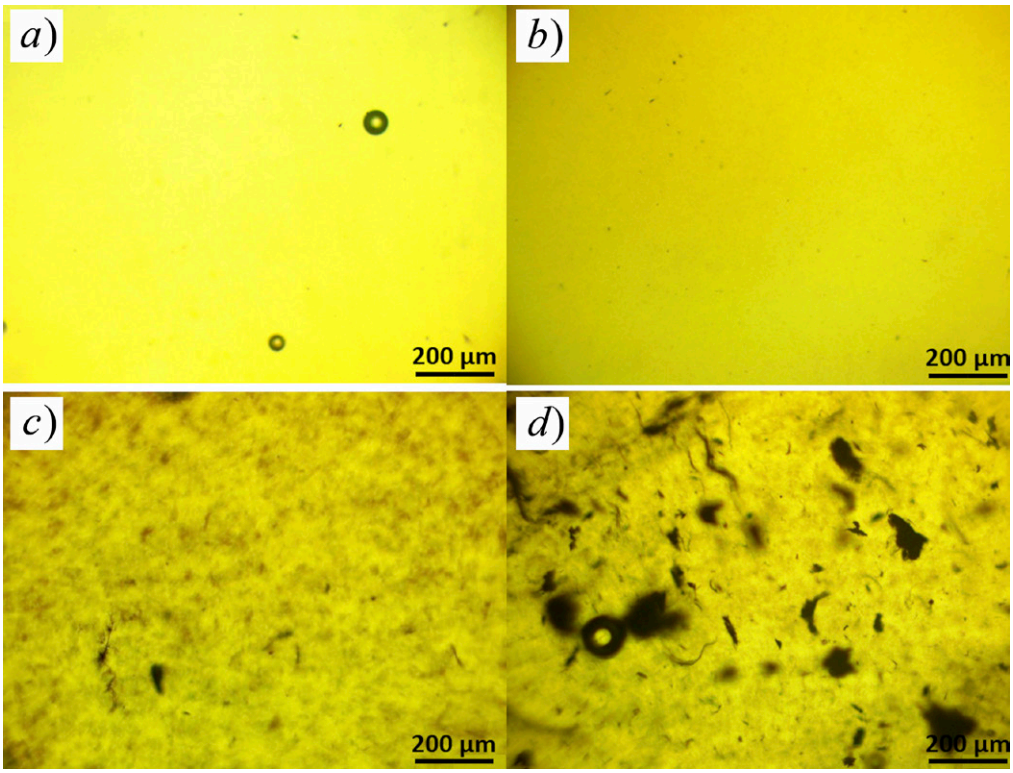

Fig. 3. Optical microphotographs of the four liquid mCNT/epoxy resin formulations with 0.1% CNT: for the best mCNT distribution (*a*), for the good CNT distribution (*b*), for the bad CNT distribution (*c*), and for the worst CNT distribution (*d*). The images were acquired in transmitted light mode from thin layers of the liquid formulations sandwiched between a microscope slide and a cover slip

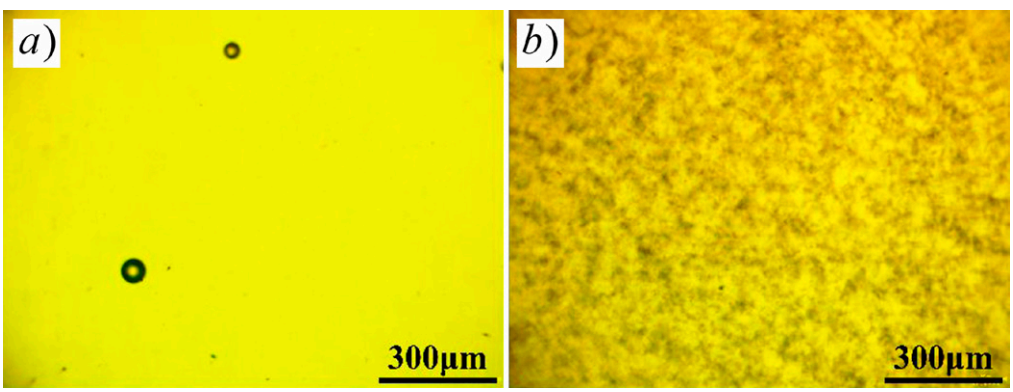

Fig. 4. Optical microphotographs of the liquid mCNT/epoxy resin formulation with 0.1% CNT (with the best CNT distribution): *a* – the as-prepared formulation immediately after the sonication; *b* – the same formulation after standing for 30 min at 80 °C. The images were acquired in transmitted light from thin layers of the liquid formulations sandwiched between a microscope slide and a cover slip

The optical microscopy findings are confirmed by the SEM images taken from the fracture surfaces of the solid polymer composites (Fig. 5). The 0.1-best sample had single CNT bundles (Fig. 5, *a*) protruding from the polymer matrix. The bundles did not split into individual CNTs. These observations further validate that a mCNT bundle is the

fundamental unit of the conductive inclusions in the composite. Besides single bundles (Fig. 4, *a*), many small-sized aggregates consisting of 3–5 bundles were detected. The 0.1-worst sample had numerous large aggregates, each comprising numerous bundles (Fig. 5, *b*). The bundles were located at different angles and distances from each other. Some of them merged with each other at certain points and diverged at others, thus constituting a percolated network. The aggregate visible in Fig. 4, *b* is most likely only the tip of the iceberg, with the main part lying under the fracture surface.

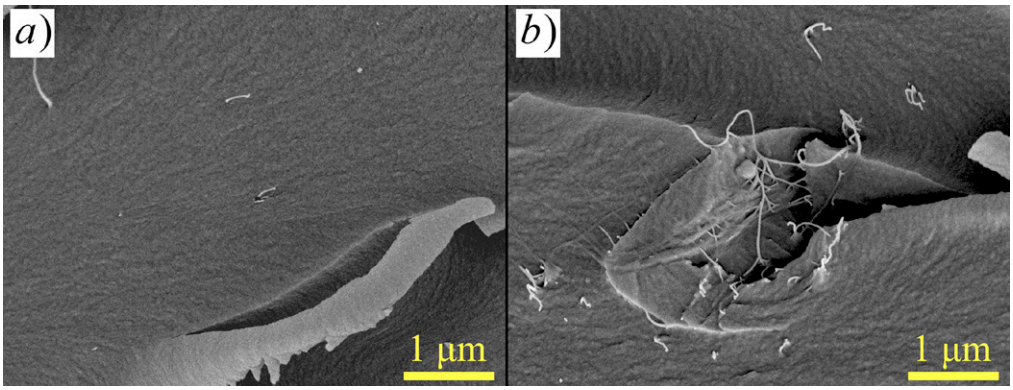

Fig. 5. SEM images of the fracture surfaces in the mCNT/epoxy composites: the samples with the best 0.1% CNT (*a*) and worst 0.1% CNT (*b*) distributions

The permittivity of the solid composites prepared from the four liquid formulations (Fig. 6) differs dramatically, even though they had the same content (0.1%) of the conductive filler. The obtained permittivity vales were contrary to what one might expect: the samples with better CNT distribution had a lower permittivity, and vice versa. For the 0.1-best sample, the real part of the complex permittivity (Fig. 6, *a*) changed from 6.5 Hz at the high-frequency end through 17 Hz at the low-frequency end, i.e., it was only slightly higher than the permittivity of the neat epoxy polymer, which is ~3 in the full tested frequency range. At the same time, the permittivity of the 0.1% worst sample with large aggregates varied from 15.6 through 482 Hz. The curves for the 0.1-good and 0.1-bad samples are positioned between the curves of the two extreme samples.

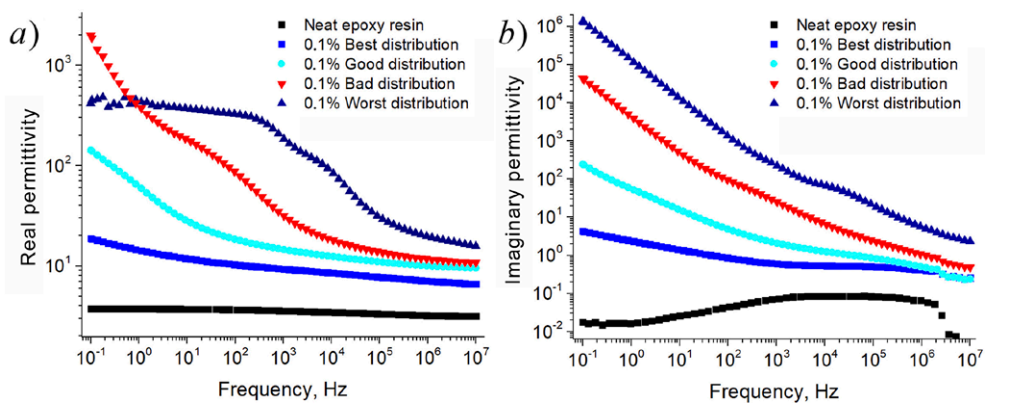

Fig. 6. Real (*a*) and imaginary (*b*) parts of the complex permittivity for the four samples with different level of CNT aggregation (CNT content 0.1%)

It is important that the differences between the samples are more pronounced in the low-frequency part of the tested region. In the high-frequency end, the differences are not that distinct: the real part values for the samples with the best and worst mCNT distributions were 6.5 and 15.6, respectively (Fig. 6, *a*). Nevertheless, at a frequency of 10^3 Hz, the respective values were 9.2 and 194, with a 21-fold difference between the two samples. Finally, at a frequency of 10^1 Hz, the permittivity values for the 0.1-best, 0.1-good, 0.1-bad, and 0.1-worst samples were 11.6, 27.3, 179.5, and 370.5, respectively.

The real part curve for the 0.1-best sample is almost flat, with only a slight increase towards frequencies lower than 10 Hz. In contrast, the 0.1-good sample has a more pronounced increase. The 0.1-bad sample exhibits an additional permittivity dispersion within the frequencies of 10^3–10^2 Hz. For the 0.1-worst sample, there are two permittivity dispersion ranges in the middle of the tested frequency interval. Therefore, the permittivity dispersion range gradually shifts toward higher frequencies in the 0.1-best to 0.1-worst samples.

The imaginary part of complex permittivity (Fig. 6, *b*) increases notably toward the low-frequency end of the spectra, which is especially evident in the aggregated samples. For these samples at frequencies < 10^3 Hz, the imaginary part surpasses the real part. The loss peaks are distinguishable, but they are partially obscured by the strong contribution of DC conductivity.

At higher mCNT loadings, it becomes more difficult to precisely control the mCNTs distribution in the matrix, if compared with 0.1% mCNT. Even at 0.2% mCNT, a sample completely free from aggregates cannot be obtained. As mCNT loadings increase, the difficulties scale up. Thus, for 0.2% and 0.5% mCNT, only two (not four) types of samples, with more and less uniform distribution, were prepared: the ones with "good" and "bad" mCNT distribution. At 0.5% mCNT, the uniform non-aggregated state cannot be achieved. Here, "0.5-good" means "intended good," i.e., prepared according to the procedures for uniform samples. The measured permittivity values for the two 0.2% mCNT and two 0.5% mCNT samples are shown in Fig. 7.

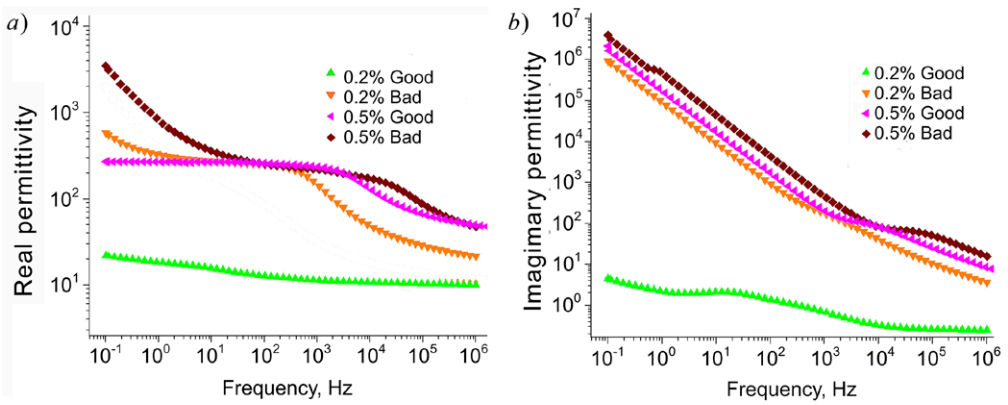

Fig. 7. Real (*a*) and imaginary (*b*) parts of the complex permittivity for the samples with 0.2% and 0.5% CNT content with two different levels of aggregation for each

For the samples with 0.2% mCNT, the same trend was observed as for 0.1% mCNT. In the 0.2-good samples, the real part of permittivity gradually changes from 10.2 to 21.4 (Fig. 7, *a*), which is similar to what was observed in the 0.1-best sample. The permittivity values of the 0.2-bad sample lie in the range of 23–286. Thus, at 0.2% loading, the two samples with different aggregation degree still differ significantly. However, at 0.5% mCNT, the difference between the two samples is minimal. In the frequency range of 10^2–10^6 Hz, the two curves almost overlap (Fig. 7, *a*). This is because mCNTs inevitably aggregate at 0.5% loading. This is why the samples with the filler content higher than 0.5% were not considered.

In our previous work [53], composites prepared from the raw non-modified Tuball CNTs and a silicon elastomer as a non-conductive matrix were tested. The CNTs in these composites were highly aggregated due to the low affinity toward the matrix. The size and shape of the CNT aggregates were similar to those in Fig. 3, *c* and *d*. The permittivity matched the values registered in this study for the highly aggregated samples. The following two conclusions were made based on the above results: first, the oxidative modification of CNTs does not significantly degrade their conductivity; second, the choice of the polymer matrix is not essential for the conductive properties of composites. The second conclusion is particularly important. The interfacial structures in the two systems, mCNT/epoxy and CNT/silicon, must be different. However, both composites exhibit similar permittivity values, which depend only on the distribution of nanotubes in the matrix. So, an "interface effect" described by some researchers has no significant influence on permittivity.

In Fig. 8, the data collected for the samples with uniform and non-uniform mCNT distribution are presented separately. For the samples (Fig. 8, *a*, *b*) with a uniform mCNT distribution, the permittivity values differ considerably between the 0.2% and 0.5% loadings. In the light of the percolation theory, it could be interpreted as a threshold between the two filling fractions. However, the new findings suggest that this sharp increase stems from the different uniformity of the two samples: the non-aggregated state in the 0.2-good sample and the aggregated state in the 0.5-good sample. The difference between the 0.1% and 0.2% mCNT samples is minimal. With a more or less uniform dispersion of mCNTs, a 2x increase in the filler content only slightly affects the permittivity values. The 0.2-good sample demonstrates significantly lower values in the real part than the 0.1-worst and 0.1-bad samples throughout the entire frequency range. Thus, the sample with a higher conductive filler content is less conductive than the samples with a lower filler content.

For the aggregated samples (Fig. 8, *c*, *d*), the difference between all the three loadings is not very pronounced, thereby indicating that the number or density of the aggregates in the matrix does not strongly affect the permittivity in the tested frequency range. The difference between the three aggregated samples intensifies toward the high-frequency end of the tested range, demonstrating the role of the overall filler content.

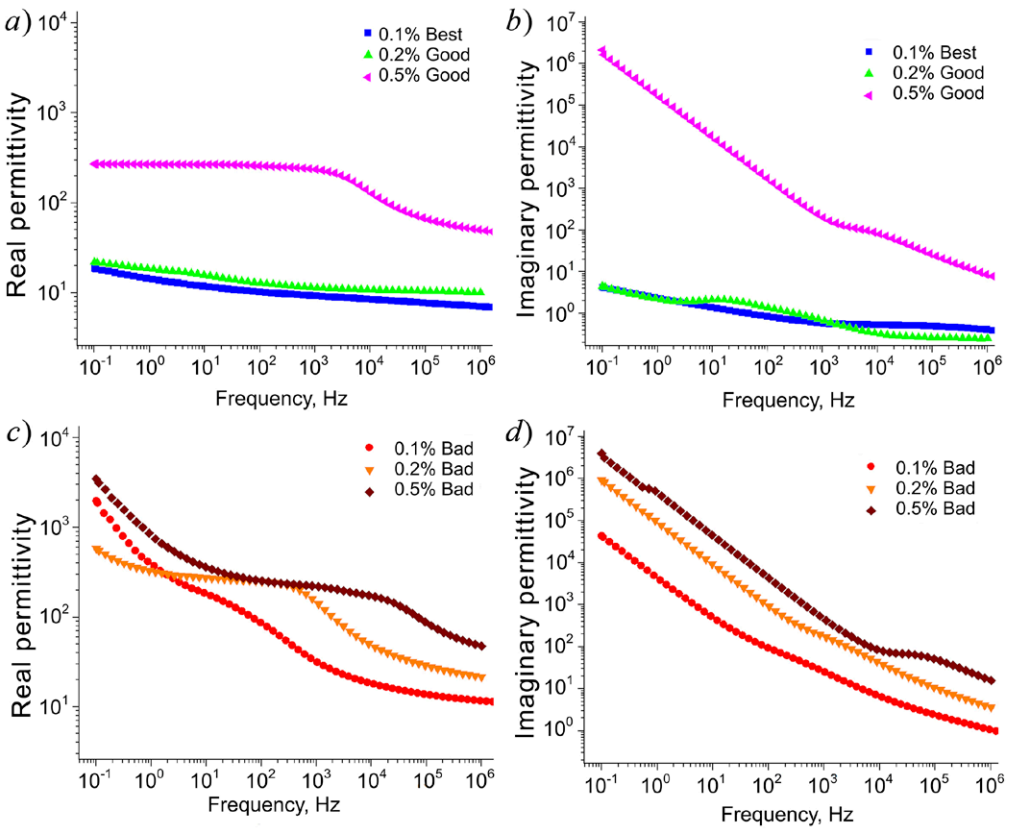

Fig. 8. Permittivity values for the samples with good (*a*, *b*) and bad (*c*, *d*) mCNT distribution at three different loadings. (*a*, *c*) The real and (*b*, *d*) the imaginary parts of the complex permittivity

The leading experts in the field admit that the actual physics behind the polarization mechanism in composite materials remains poorly understood [1]. This is especially true for systems where the filler particles are not uniform in size and shape to be easily modeled mathematically. The problem is even more challenging for systems like CNT/polymer, in which the values of many geometical parameters (the size of CNT aggregates, the thickness of the insulator layer between CNT bundles, the shape of the percolative network within CNT aggregates, etc.) vary widely. This study limits its scope to the most straightforward and obvious observations concerning the polarization mechanism. The loss peaks of the imaginary part curves can signify an interfacial capacitance in the series with resistance, i.e., the bulk polymer regions, which constitutes the basis of interfacial polarization, often referred to as the Maxwell–Wagner polarization [1]. The strong permittivity dispersion observed in the aggregated composites at frequencies < 10 Hz points to long relaxation times, which in turn can be interpreted as the hindered charge transfer within a polarizable conductive inclusion. The difficulty of the charge transfer can be explained by the presence of a thin polymer layer between the two conductors. In our systems, such a layer is likely to be present within the CNT aggregates due to the strong adhesion of epoxy resin to mCNTs. The significant permittivity dispersion in the low-frequency end of the tested region can be tentatively attributed to the polarization between the two separated parts of the same large aggregate. This explanation is indirectly con-

firmed by the notable increase of the imaginary part in the low-frequency end due to the contribution of DC conductivity.

The dispersion of permittivity at relatively high frequencies in the middle of the tested frequency range arised from the polarization within the CNT aggregates. However, the distinction between polarizable units is rather arbitrary. The size of the CNT aggregates, the distance between the bundles within the CNT aggregate, and the distance between the neighboring CNT aggregates within the same sample varied in a broad continuous range. These variations determined the frequencies at which the permittivity dispersion occured.

Regardless of the mechanistic explanations, our findings reliably indicate that the polarization observed in the tested frequency range occurred predominantly due to the presence of the CNT aggregates. Additionally, the permittivity values, higher than those for the neat resin, recorded for the 0.1-best sample, are most likely due to the presence of small CNT aggregates, each comprising 3–5 bundles, which were observed based on the SEM images of the fracture surfaces. Single CNT bundles separated from each other by thick insulator layer would not contribute to the permittivity values within the tested frequency range because of the capacitance being inversely proportional to the distance between the capacitor plates. In other words, when the insulator layer between the two conductors is thin, an aggregate functions as a microcapacitor. Thus, our results further validate the microcapacitor model and should be discussed in terms of the Maxwell–Wagner polarization.

The role played by CNTs aggregates in the polarization process implies that the size of the dielectric polymer components can be reduced, in theory, to the size of a few CNTs, i.e., to tens of micrometers. This paves the way for the potential miniaturization of the components. An ideal microcapacitor would consist of two parallel CNTs arranged at a properly calculated distance.

The conductive properties of composite materials have been described using various approaches (see Introduction). Our data prove that the permittivity of CNT/polymer composites (at all the studied frequencies) depends mostly on the distribution of CNTs in the matrix. The aggregation of CNTs in the matrix should be considered as the key factor influencing the conductive properties of CNT/polymer composites. As a short example, in [30], relatively low permittivity values (69.7 for the 4% CNT content, measured at 1 kHz) were registered for the MWCNT/PVDF composite, while similar systems normally exhibit much higher permittivity values up to 10 000 [27, 32]. The lower permittivity registered in [30] can be explained by the uniform distribution of CNTs in the matrix, attained by the non-covalent functionalization, but not via an "interface effect" as one might suggest.

The perlocation theory is only valid for ideal composites with the filler having completely uniform particles. Otherwise, models based on the geometrical and statistical considerations make little sense. In reality, samples with a lower filler content (such as the 0.1-worst sample) might have higher permittivity values than those with a larger filler content (such as the 0.2-good sample). Thus, mathematical approaches like the power laws are of little help here or at least have some critical limitations. The revealed "aggregation effect" explains the inconsistensies in the available literature data on the conductive properties of CNT/polymer composites. Many earlier results, especially those concerning the percolation threshold values, may require a reconsideration in the light of the findings of this study.

Conclusions

A new method for manufacturing CNT/epoxy resin composites with a completely uniform distribution of CNTs in the matrix was developed. With the Tuball CNTs used in this study, this is possible up to the CNT content of 0.2%. The method allows to control the levels of uniformity/aggregation in a broad range, while the CNT content of composites remains constant. The conductive properties of the obtained composites were measured at frequencies from 10^{-1} to 10^{7} Hz. Depending on the levels of CNT aggregation, the permittivity values varied widely, even though the content of the conductive filler did not change. In addition, they were inversely related to the degree of CNT uniformity in the matrix. The aggregated sample with 0.1% CNT content was characterized by the highest permittivity (up to 482 at the low-frequency end), and the sample with CNTs distributed uniformly had a very low permittivity (< 17). At a frequency of 10^{1} Hz, the permittivity values for the 0.1-best, 0.1-good, 0.1-bad, and 0.1-worst samples were 11.6, 27.3, 179.5, and 370.5, respectively. The same trend was observed with 0.2% CNT. At higher loadings, it is impossible to prepare non-aggregated samples, and the difference between the samples with a more or less uniform CNT distribution is minimal. For the aggregated samples within the 0.1–0.5% filling fractions, the permittivity is determined more by their aggregation than the overall CNT content. Thus, the sample with 0.2% CNTs distributed uniformly exhibited a significantly lower permittivity compared to the aggregated sample with 0.1% CNT throughout the entire tested frequency range. Our data strongly suggest that the degree of CNT aggregation is the key factor to be taken into account when interpreting the conductive properties of CNT/polymer composites. Other factors, such as non-covalent functionalization of CNTs, might only contribute to the uniformity/aggregation of composites, which in turn affects their permittivity. Therefore, although the power laws can be effective, using them to study and manufacture CNT/polymer composites is associated with critical limitations.

Acknowledgments. This study was supported by Russian Science Foundation (project no. 21-73-20024).

Conflicts of Interest. The authors declare no conflicts of interest.

References

1. Jonscher A.K. Dielectric relaxation in solids. *J. Phys. D: Appl. Phys.*, 1999, vol. 32, no. 14, pp. R57–R70. https://doi.org/10.1088/0022-3727/32/14/201.
2. Ajayan P.M., Tour J.M. Nanotube composites. *Nature*, 2007, vol. 447, no. 7148, pp. 1066–1068. https://doi.org/10.1038/4471066a.
3. Terrones M., Martín O., González M., Pozuelo J., Serrano B., Cabanelas J.C., Vega-Díaz S.M., Baselga J. Interphases in graphene polymer-based nanocomposites: Achievements and challenges. *Adv. Mater.*, 2011, vol. 23, no. 44, pp. 5302–5310. https://doi.org/10.1002/adma.201102036.
4. Baughman R.H., Zakhidov A.A., de Heer W.A. Carbon nanotubes – the route toward applications. *Science*, 2002, vol. 297, no. 5582, pp. 787–792. https://doi.org/10.1126/science.1060928.
5. Coleman J., Curran S., Dalton A.B., Davey A.P., McCarthy B., Blau W., Barklie R.C. Percolation-dominated conductivity in a conjugated-polymer-car-

bon-nanotube composite. *Phys. Rev. B*, 1998, vol. 58, no. 12, pp. R7492–R7495. https://doi.org/10.1103/PhysRevB.58.R7492.

6. Grimes C.A., Mungle C., Kouzoudis D., Fang S., Eklund P.C. The 500 MHz to 5.50 GHz complex permittivity spectra of single-wall carbon nanotube-loaded polymer composites. *Chem. Phys. Lett.*, 2000, vol. 319, nos. 5–6, pp. 460–464. https://doi.org/10.1016/S0009-2614(00)00196-2.
7. Wu J., Kong L. High microwave permittivity of multiwalled carbon nanotube composites. *Appl. Phys. Lett.*, 2004, vol. 84, no. 24, pp. 4956–4958. https://doi.org/10.1063/1.1762693.
8. Logakis E., Pandis Ch., Peoglos V., Pissis P., Pionteck J., Pötschke P., Mičušík M., Omastová M. Electrical/dielectric properties and conduction mechanism in melt processed polyamide/multi-walled carbon nanotubes composites. *Polymer*, 2009, vol. 50, no. 21, pp. 5103–5111. https://doi.org/10.1016/j.polymer.2009.08.038.
9. Dang Z.-M., Wang L., Yin Y., Zhang Q., Lei Q.-Q. Giant dielectric permittivities in functionalized carbon-nanotube/electroactive-polymer nanocomposites. *Adv. Mater.*, 2007, vol. 19, no. 6, pp. 852–857. https://doi.org/10.1002/adma.200600703.
10. Yuan J.-K., Yao S.-H., Dang Z.-M., Sylvestre A., Genestoux M., Bai J. Giant dielectric permittivity nanocomposites: Realizing true potential of pristine carbon nanotubes in polyvinylidene fluoride matrix through an enhanced interfacial interaction. *J. Phys. Chem. C*, 2011, vol. 115, no. 13, pp. 5515–5521. https://doi.org/10.1021/jp1117163.
11. Dimiev A., Lu W., Zeller K., Crowgey B., Kempel L.C., Tour J.M. Low-loss, high-permittivity composites made from graphene nanoribbons. *ACS Appl. Mater. Interfaces*, 2011, vol. 3, no. 12, pp. 4657–4661. https://doi.org/10.1021/am201071h.
12. Dimiev A., Zakhidov D., Genorio B., Oladimeji K., Crowgey B., Kempel L., Rothwell E.J., Tour J.M. Permittivity of dielectric composite materials comprising graphene nanoribbons. The effect of nanostructure. *ACS Appl. Mater. Interfaces*, 2013, vol. 5, no. 15, pp. 7567–7573. https://doi.org/10.1021/am401859j.
13. Lounev I.V, Musin D.R., Dimiev A.M. New details to relaxation dynamics of dielectric composite materials comprising longitudinally opened carbon nanotubes. *J. Phys. Chem. C*, 2017, vol. 121, no. 41, pp. 22995–23001. https://doi.org/10.1021/acs.jpcc.7b08406.
14. Dang Z.-M., Wu J.-P., Xu H.-P., Yao S.-H., Jiang M.-J., Bai J. Dielectric properties of upright carbon fiber filled poly(vinylidene fluoride) composite with low percolation threshold and weak temperature dependence. *Appl. Phys. Lett.*, 2007, vol. 91, no. 7, art. 072912. https://doi.org/10.1063/1.2770664.
15. Liu C., Zheng L., Yuan L., Guan Q., Gu A., Liang G. Origin of increasing dielectric constant at lower percolation threshold through controlling spatial distribution of carbon nanotubes in epoxy resin with microwave-assisted thermal curing technique. *J. Phys. Chem. C*, 2016, vol. 120, no. 50, pp. 28875–28885. https://doi.org/10.1021/acs.jpcc.6b10567.
16. Bal S., Samal S.S. Carbon nanotube reinforced polymer composites—a state of the art. *Bull. Mater. Sci.*, 2007, vol. 30, no. 4, pp. 379–386. https://doi.org/10.1007/s12034-007-0061-2.
17. Bergman D.J., Imry Y. Critical behavior of the complex dielectric constant near the percolation threshold of a heterogeneous material. *Phys. Rev. Lett.*, 1977, vol. 39, no. 19, pp. 1222–1225. https://doi.org/10.1103/PhysRevLett.39.1222.
18. Bánhegyi G. Comparison of electrical mixture rules for composites. *Colloid Polym. Sci.*, 1986, vol. 264, no. 12, pp. 1030–1050. https://doi.org/10.1007/BF01410321.
19. Nan C.-W. Physics of inhomogeneous inorganic materials. *Prog. Mater. Sci.*, 1993, vol. 37, no. 1, pp. 1–116. https://doi.org/10.1016/0079-6425(93)90004-5.
20. Feldman Y., Puzenko A., Ryabov Y. Dielectric relaxation phenomena in complex materials. In: Coffey W.T., Kalmykov Y.P. (Eds.) *Fractals, Diffusion, and Relaxation in*

Disordered Complex Systems. Hoboken, NJ, Wiley-Interscience, 2006, pp. 1–125. http://dx.doi.org/10.1002/0471790265.ch1.

21. Cametti C. Dielectric spectra of ionic water-in-oil microemulsions below percolation: Frequency dependence behavior. *Phys. Rev. E*, 2010, vol. 81, no. 3, art. 031403. https://doi.org/10.1103/PhysRevE.81.031403.
22. Li J., Ma P.C., Chow W.S., To C.K., Tang B.Z., Kim J.-K. Correlations between percolation threshold, dispersion state, and aspect ratio of carbon nanotubes. *Adv. Funct. Mater.*, 2007, vol. 17, no. 16, pp. 3207–3215. https://doi.org/10.1002/adfm.200700065.
23. Wang D., Zhang X., Zha J.W., Zhao J.-W., Zhao J., Dang Z.-M., Hu G.-H. Dielectric properties of reduced graphene oxide/polypropylene composites with ultralow percolation threshold. *Polymer*, 2013, vol. 54, no. 7, pp. 1916–1922. https://doi.org/10.1016/j.polymer.2013.02.012.
24. Moharana S., Mahaling R.N. Silver (Ag)-graphene oxide (GO) – poly (vinylidene fluoride-co-hexafluoropropylene) (PVDF-HFP) nanostructured composites with high dielectric constant and low dielectric loss. *Chem. Phys. Lett.*, 2017, vol. 680, pp. 31–36. https://doi.org/10.1016/j.cplett.2017.05.018.
25. He F., Lau S., Chan H.L., Fan J. High dielectric permittivity and low percolation threshold in nanocomposites based on poly(vinylidene fluoride) and exfoliated graphite nanoplates. *Adv. Mater.*, 2009, vol. 21, no. 6, pp. 710–715. https://doi.org/10.1002/adma.200801758.
26. Wan Y.-J., Yang W.-H., Yu S.-H., Sun R., Wong C.-P., Liao W.-H. Covalent polymer functionalization of graphene for improved dielectric properties and thermal stability of epoxy composites. *Compos. Sci. Technol.*, 2016, vol. 122, pp. 27–35. https://doi.org/10.1016/j.compscitech.2015.11.005.
27. Yuan J.-K., Li W.-L., Yao S.-H., Lin Y.-Q., Sylvestre A., Bai J. High dielectric permittivity and low percolation threshold in polymer composites based on SiC-carbon nanotubes micro/nano hybrid. *Appl. Phys. Lett.*, 2011, vol. 98, no. 3, art. 032901. https://doi.org/10.1063/1.3544942.
28. Tong W., Zhang Y., Zhang Q., Luan X., Duan Y., Pan S., Lv F., An Q. Achieving significantly enhanced dielectric performance of reduced graphene oxide/polymer composite by covalent modification of graphene oxide surface. *Carbon*, 2015, vol. 94, pp. 590–598. https://doi.org/10.1016/j.carbon.2015.07.005.
29. Khamidullin T., Lounev I., Solodov A., Vakhitov I., Hashemi S.A., Dimiev A.M. Graphene oxide–epoxy composites with induced anisotropy of electrical properties. *J. Phys. Chem. C*, 2021, vol. 125, no. 48, pp. 26823–26831. https://doi.org/10.1021/acs.jpcc.1c07645.
30. Luo H., Wu Z., Chen C., Ma C., Zhou K., Zhang D. Methoxypolyethylene glycol functionalized carbon nanotube composites with high permittivity and low dielectric loss. *Composites, Part A*, 2016, vol. 86, pp. 57–65. https://doi.org/10.1016/j.compositesa.2016.04.001.
31. Li Q., Xue Q., Hao L., Gao X., Zheng Q. Large dielectric constant of the chemically functionalized carbon nanotube/polymer composites. *Compos. Sci. Technol.*, 2008, vol. 68, nos. 10–11, pp. 2290–2296. https://doi.org/10.1016/j.compscitech.2008.04.019.
32. Shang S., Tang C., Jiang B., Song J., Jiang B., Zhao K., Liu Y., Wang X. Enhancement of dielectric permittivity in carbon nanotube/polyvinylidene fluoride composites by constructing of segregated structure. *Compos. Commun.*, 2021, vol. 25, art. 100745. https://doi.org/10.1016/j.coco.2021.100745.
33. Sun D., Zhou Z., Chen G.-X., Li Q. Regulated dielectric loss of polymer composites from coating carbon nanotubes with a cross-linked silsesquioxane shell through free-radical polymerization. *ACS Appl. Mater. Interfaces*, 2014, vol. 6, no. 21, pp. 18635–18643. https://doi.org/10.1021/am503633t.

34. Amirova L., Surnova A., Balkaev D., Musin D., Amirov R., Dimiev A.M. Homogeneous liquid phase transfer of graphene oxide into epoxy resins. *ACS Appl. Mater. Interfaces*, 2017, vol. 9, no. 13, pp. 11909–11917. https://doi.org/10.1021/acsami.7b02243.

35. Dimiev A.M., Surnova A., Lounev I., Khannanov A. Intrinsic insertion limits of graphene oxide into epoxy resin and the dielectric behavior of composites comprising truly 2D structures. *J. Phys. Chem. C*, 2019, vol. 123, no. 6, pp. 3461–3468. https://doi.org/10.1021/acs.jpcc.8b07450.

36. Surnova A., Balkaev D., Musin D., Amirov R., Dimiev A.M. Fully exfoliated graphene oxide accelerates epoxy resin curing, and results in dramatic improvement of the polymer mechanical properties. *Composites, Part B*, 2019, vol. 162, pp. 685–691. https://doi.org/10.1016/j.compositesb.2019.01.020.

37. Dimiev A.M., Lounev I., Khamidullin T., Surnova A., Valimukhametova A., Khannanov A. Polymer composites comprising single-atomic-layer graphenic conductive inclusions and their unusual dielectric properties. *J. Phys. Chem. C*, 2020, vol. 124, no. 25, pp. 13715–13725. https://doi.org/10.1021/acs.jpcc.0c02208.

38. Dimiev A.M., Khannanov A., Vakhitov I., Kiiamov A., Shukhina K., Tour J.M. Revisiting the mechanism of oxidative unzipping of multiwall carbon nanotubes to graphene nanoribbons. *ACS Nano*, 2018, vol. 12, no. 4, pp. 3985–3993. https://doi.org/10.1021/acsnano.8b01617.

39. Hummers W.S.Jr., Offeman R.E. Preparation of graphitic oxide. *J. Am. Chem. Soc.*, 1958, vol. 80, no. 6, p. 1339. https://doi.org/10.1021/ja01539a017.

40. Feicht P., Biskupek J., Gorelik T.E., Renner J., Halbig C.E., Maranska M., Puchtler F., Kaiser U., Eigler S. Brodie's or Hummers' method: Oxidation conditions determine the structure of graphene oxide. *Chem. – Eur. J.*, 2019, vol. 25, no. 38, pp. 8955–8959. https://doi.org/10.1002/chem.201901499.

41. Dimiev A.M., Shukhina K., Khannanov A. Mechanism of the graphene oxide formation: The role of water, "reversibility" of the oxidation, and mobility of the C–O bonds. *Carbon*, 2020, vol. 166, pp. 1–14. https://doi.org/10.1016/j.carbon.2020.05.005.

42. Kosynkin D., Higginbotham A.L., Sinitskii A., Lomeda J.R., Dimiev A., Price B.K., Tour J.M. Longitudinal unzipping of carbon nanotubes to form graphene nanoribbons. *Nature*, 2009, vol. 458, no. 7240, pp. 872–876. https://doi.org/10.1038/nature07872.

43. Eigler S., Dimiev A.M. Characterization techniques. In: Dimiev A.M., Eigler S. (Eds.) *Graphene Oxide: Fundamentals and Applications*. Chichester, Wiley, 2016, pp. 85–120. https://doi.org/10.1002/9781119069447.ch3.

44. Shayimova J., Amirov R.R., Iakunkov A., Talyzin A., Dimiev A.M. Carboxyl groups do not play the major role in binding metal cations by graphene oxide. *Phys. Chem. Chem. Phys.*, 2021, vol. 23, no. 32, pp. 17430–17439. https://doi.org/10.1039/D1CP01734A.

45. Dimiev A.M., Bachilo S.M., Saito R., Tour J.M. Reversible formation of ammonium persulfate/sulfuric acid graphite intercalation compounds and their peculiar Raman spectra. *ACS Nano*, 2012, vol. 6, no. 9, pp. 7842–7849. https://doi.org/10.1021/nn3020147.

46. Cançado L.G., Jorio A., Martins Ferreira E.H., Stavale F., Achete C.A., Capaz R.B., Moutinho M.V.O., Lombardo A., Kulmala T.S., Ferrari A.C. Quantifying defects in graphene via Raman spectroscopy at different excitation energies. *Nano Lett.*, 2011, vol. 11, no. 8, pp. 3190–3196. https://doi.org/10.1021/nl201432g.

47. Lucchese M.M., Stavale F., Martins Ferreira E.H., Vilani C., Moutinho M.V.O., Capaz R.B., Achete C.A., Jorio A. Quantifying ion-induced defects and Raman relaxation length in graphene. *Carbon*, 2010, vol. 48, no. 5, pp. 1592–1597. https://doi.org/10.1016/j.carbon.2009.12.057.

48. King A.A.K., Davies B.R., Noorbehesht N., Newman P., Church T.L., Harris A.T., Razal J.M., Minett A.I. A new Raman metric for the characterisation of graphene oxide and its derivatives. *Sci. Rep.*, 2016, vol. 6, no. 1, art. 19491. https://doi.org/10.1038/srep19491.

49. Kleshch V.I., Eremina V.A., Serbun P., Orekhov A.S., Lützenkirchen-Hecht D., Obraztsova E.D., Obraztsov A.N. A comparative study of field emission from semiconducting and metallic single-walled carbon nanotube planar emitters. *Phys. Status Solidi B*, 2018, vol. 255, no. 1, art. 1700268. https://doi.org/10.1002/pssb.201700268.

50. Krestinin A.V, Dremova N.N., Knerel'man E.I., Blinova L.N., Zhigalina V.G., Kiselev N.A. Characterization of SWCNT products manufactured in Russia and the prospects for their industrial application. *Nanotechnol. Russ.*, 2015, vol. 10, nos. 7–8. pp. 537–548. https://doi.org/10.1134/S1995078015040096.

51. Turek E., Wasiak T., Stando G., Janas D. Probing the mechanics of aqueous two-phase extraction using large diameter single-walled carbon nanotubes. *Nanotechnology*, 2018, vol. 29, no. 40, art. 405704. https://doi.org/10.1088/1361-6528/aad359.

52. Khamidullin T., Galyaltdinov S., Valimukhametova A., Brusko V., Khannanov A., Maat S., Kalinina I., Dimiev A.M. Simple, cost-efficient and high throughput method for separating single-wall carbon nanotubes with modified cotton. *Carbon*, 2021, vol. 178, pp. 157–163. https://doi.org/10.1016/j.carbon.2021.03.003.

53. Galyaltdinov S., Lounev I., Khamidullin T., Hashemi S.A., Nasibulin A. Dimiev A.M. High permittivity polymer composites on the basis of long single-walled carbon nanotubes: The role of the nanotube length. *Nanomaterials*, 2022, vol. 12, no. 19, art. 3538. https://doi.org/10.3390/nano12193538.

Received March 22, 2024
Accepted April 17, 2024

Khamidullin Timur Lenarovich, PhD Student, Department of Physical Chemistry, A.M. Butlerov Institute of Chemistry

Kazan Federal University
ul. Kremlevskaya, 18, Kazan, 420008 Russia
E-mail: *TiLKhamidullin@kpfu.ru*

Lounev Ivan Vladimirovich, PhD in Physics, Associate Professor, Senior Research Fellow, Department of Quantum Electronics and Radiospectroscopy, Institute of Physics

Kazan Federal University
ul. Kremlevskaya, 18, Kazan, 420008 Russia
E-mail: *lounev75@mail.ru*

Sattarov Sergey Abudievich, PhD in Physics, Associate Professor, Department of Radioelectronics

Jizzakh Polytechnical Institute
pr. I. Karimova, 4, Jizzakh, 130100 Republic of Uzbekistan
E-mail: *jizpi_sattarov@list.ru*

Dimiev Ayrat Maratovich, Doctor of Chemistry, Leading Research Fellow, Laboratory for Advanced Carbon Nanomaterials, A.M. Butlerov Institute of Chemistry

Kazan Federal University
ul. Kremlevskaya, 18, Kazan, 420008 Russia
E-mail: *AMDimiev@kpfu.ru*

ОРИГИНАЛЬНАЯ СТАТЬЯ

УДК 546.05 doi: 10.26907/2542-064X.2024.2.210-228

Аномальные проводящие свойства полимерных композитов с углеродными нанотрубками: неуниверсальность степенного закона

Т.Л. Хамидуллин[1], И.В. Лунев[1], С.А. Саттаров[2], А.М. Димиев[1]

[1] Казанский Федеральный Университет, г. Казань, 420008, Россия
[2] Джизакский политехнический институт, г. Джизак, 130100, Узбекистан

Аннотация

Проводящие свойства полимерных композитов с углеродными нанотрубками (УНТ) хорошо известны и подробно описаны в литературе. Однако влияние степени распределения УНТ в матрице на поляризацию композитов до конца не изучено. Добиться равномерного распределения УНТ в полимерах практически невозможно, поэтому в большинстве имеющихся публикаций рассматриваются условия, при которых УНТ неизбирательно агрегированы. В статье представлен новый метод смешения УНТ с эпоксидной смолой для получения композитных материалов с различной однородностью/агрегацией УНТ в матрице при одинаковом содержании наполнителя. Проведенный эксперимент показал, что значения диэлектрической проницаемости обратно пропорциональны однородности композита, при этом самые низкие показатели проницаемости были выявлены в наиболее однородных образцах, и наоборот. При 0.1% УНТ, значения проводимости в реальной части составили 6.6 и 16.2 при 10^7 Гц и 11.6 и 370.5 при 10^1 Гц для наиболее однородных и наиболее агрегированных образцов соответственно. Показано, что в диапазоне концентраций наполнителя 0.1–0.5 % проводящие свойства зависели главным образом от распределения УНТ, а не от их содержания. Так, во всем диапазоне частот однородный образец с 0.2% УНТ демонстрировал значительно меньшую проницаемость, чем агрегированный образец с 0.1% УНТ. Эти результаты свидетельствуют о необходимости учета фактора агрегации, а также ставят под сомнение универсальность теории перколяции и степенных законов. Физическую суть наблюдаемого явления лучше всего объясняет модель микроконденсаторов, или поляризация Максвелла-Вагнера. Полученные данные, вероятно, потребуют пересмотра многих существующих представлений в области использования углеродных наноматериалов.

Ключевые слова: эпоксидные композиты, углеродные нанотрубки, межфазная поляризация, проводимость, агрегация, модель микроконденсаторов

Благодарности. Работа выполнена при поддержке Российского научного фонда (проект № 21-73-20024).

Конфликт интересов. Авторы заявляют об отсутствии конфликта интересов.

Поступила в редакцию 22.03.2024
Принята к публикации 17.04.2024

Хамидуллин Тимур Ленарович, аспирант кафедры физической химии Химического института им. А.М. Бутлерова

Казанский (Приволжский) федеральный университет
ул. Кремлевская, д. 18, г. Казань, 420008, Россия
E-mail: *TiLKhamidullin@kpfu.ru*

Лунев Иван Владимирович, кандидат физических наук, доцент, старший научный сотрудник кафедры квантовой электроники и радиоспектроскопии Института физики

Казанский (Приволжский) федеральный университет
ул. Кремлевская, д. 18, г. Казань, 420008, Россия
E-mail: *lounev75@mail.ru*

Саттаров Сергей Абудиевич, кандидат физических наук, доцент кафедры радиоэлектроники

Джизакский политехнический нститут
просп. И Каримова, д. 4, г. Джизак, 130100, Республика Узбекистан
E-mail: *jizpi_sattarov@list.ru*

Димиев Айрат Маратович, доктор химических наук, ведущий научный сотрудник лаборатории перспективных углеродных наноматериалов Химического института им. А.М. Бутлерова

Казанский (Приволжский) федеральный университет
ул. Кремлевская, д. 18, г. Казань, 420008, Россия
E-mail: *AMDimiev@kpfu.ru*

For citation: Khamidullin T.L., Lounev I.V., Sattarov S.A., Dimiev A.M. Anomalous conductive properties of polymer composites with carbon nanotubes: Why power laws are not universal. *Uchenye Zapiski Kazanskogo Universiteta. Seriya Estestvennye Nauki*, 2024, vol. 166, no. 2, pp. 210–228. https://doi.org/10.26907/2542-064X.2024.2.210-228.

Для цитирования: *Khamidullin T.L., Lounev I.V., Sattarov S.A., Dimiev A.M.* Anomalous conductive properties of polymer composites with carbon nanotubes: Why power laws are not universal // Учен. зап. Казан. ун-та. Сер. Естеств. науки. 2024. Т. 166, кн. 2. С. 210–228. https://doi.org/10.26907/2542-064X.2024.2.210-228.